NANO LETTERS

pubs.acs.org/NanoLett

# Self-Assembled Ultra-Compact Energy Storage Elements Based on Hybrid Nanomembranes

**Carlos César Bof Bufon,*,† José David Cojal González,† Dominic J. Thurmer,† Daniel Grimm,† Martin Bauer,† and Oliver G. Schmidt*,†,‡**

†Institute for Integrative Nanosciences, IFW Dresden, Helmholtz Strasse 20, 01069 Dresden, Germany, and ‡Material Systems for Nanoelectronics, Chemnitz University of Technology, Reichenhainer Strasse 70, 09107 Chemnitz, Germany

**ABSTRACT** Self-assembly methods combined with standard top-down approaches are demonstrated to be suitable for fabricating three-dimensional ultracompact hybrid organic/inorganic electronic devices based on rolled-up nanomembranes. Capacitors that are self-wound and manufactured in parallel are almost 2 orders of magnitude smaller than their planar counterparts and exhibit capacitances per footprint area of around 200 $\mu$F/cm$^2$. This value significantly exceeds that which was previously reported for metal−insulator−metal capacitors based on $Al_2O_3$, and the obtained specific energy (~0.55 Wh/kg) would allow their usage as ultracompact supercapacitors. By incorporating organic monolayers into the inorganic nanomembrane structure we can precisely control the electronic characteristics of the devices. The adaptation of the process for creating ultracompact batteries, coils and transformers is an attractive opportunity for reducing the size of energy storage elements, filters, and signal converters. These devices can be employed as implantable electronic circuits or new approaches for energy-harvesting applications. Furthermore, the incorporation of functional organic molecules gives rise to novel devices with almost limitless chemical and biological functionalities.

**KEYWORDS** Self-assembly, nanomembranes, flexible electronics, energy storage, self-assembled monolayers

Compact and efficient circuits[1] displaying complex functionalities are essential in modern electronics. Implantable autonomous devices envisioned to monitor and recover vital functions in the human body are only one example of the many devices possible that embody biological and chemical compatibility/functionality[2] combined with miniaturization of energy storage elements. Considering such a challenge, nanomembranes[3−6] consisting of different material classes (e.g., metal, oxide, semiconductor, organics) offer an attractive route toward the fabrication of more compact passive and active elements, energy storage units, sensors, and actuators.

Nowadays, self-assembly is widely accepted as a standard approach toward generating complex structures on many length scales.[7−12] A similar self-assembly process was reported nearly 100 years ago when Stoney noticed that strained metal layers spontaneously "curl up into beautiful close rolls" once they detach from their host substrate.[13] However, it was not until a decade ago that the great potential of this phenomenon was recognized as a candidate for exciting new perspectives and applications in micro- and nanotechnology.[12,14] The self-rolling of patterned thin layers elegantly combines top-down and bottom-up approaches to generate ordered micro- and nanostructured building blocks of almost arbitrary material combinations on a single chip.[15]

Applying the self-rolling technique, a fully integrative on-chip approach is obtained where the nanomembrane-based components can be fabricated in parallel using well-established semiconductor planar processing technologies. Therefore, while modern electronics keeps moving to ever new levels of miniaturization, the roll-up of hybrid nanomembranes offers a feasible route toward reducing the footprint of microcomponents in electronic circuits[10−12] as well as the incorporation of biological and chemical functionalities.[2]

The self-rolling process used to fabricate the self-wound ultracompact capacitor (UCCap) is outlined in Figure 1a−c. The process starts with the fabrication of a planar strained multilayer nanomembrane by the sequential deposition of metal and dielectric thin films on top of a sacrificial layer. The three-dimensional (3D) UCCap is self-assembled by selectively removing the sacrificial layer (see Supporting Information for more details).

The bottom metallic capacitor plate is carefully designed to provide the necessary strain to force the roll-up of the nanomembrane which then assumes a cylindrical shape. Since the rolling takes place in neutral pH and harmless aqueous media, the process is readily compatible with organic systems. The SEM image in Figure 1d−e shows self-wound ultracompact capacitors (UCCap) obtained in a controlled and reproducible fashion. The empty 2D area, which remains after the rolling-up, can be reprocessed for the generation of additional devices.

Once the capacitor layers and consequently their built-in strain are defined, the final tube diameter is precisely controlled by the nanomembrane releasing speed ($S_r$). The

* To whom correspondence should be addressed. E-mail: (C.C.B.B.) c.bufon@ifw-dresden.de; (O.G.S.) o.schmidt@ifw-dresden.de. Ph: +49 (0)351 4659 858. FAX: +49 (0)351 4659 782.

**Received for review: 03/24/2010**
**Published on Web: 06/10/2010**





DOI: 10.1021/nl1010367 | *Nano Lett.* **2010,** *10,* 2506–2510

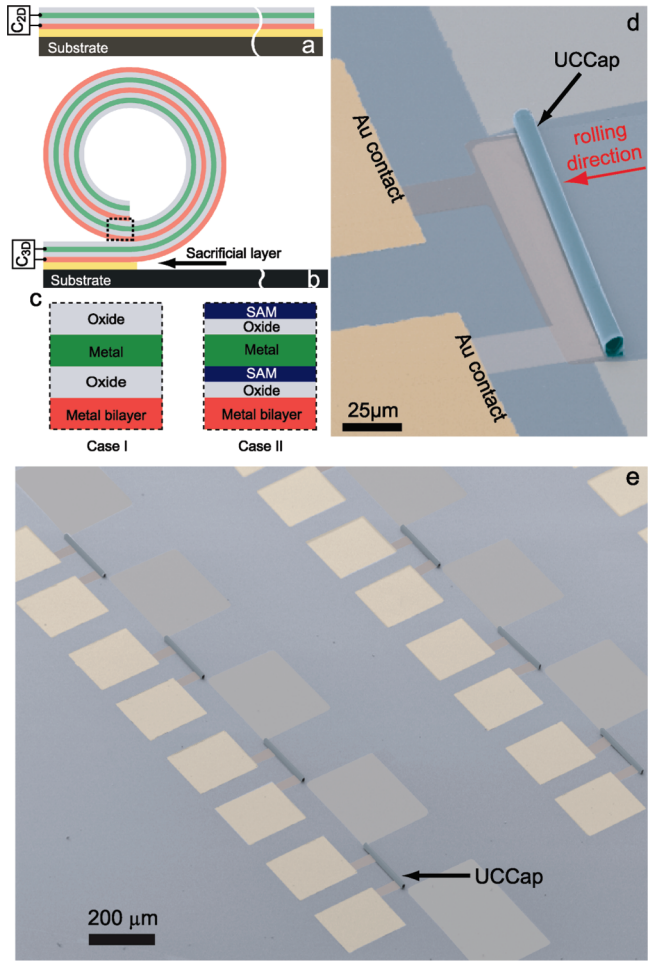


**FIGURE 1. (a) Layer sequence used to create the nanomembrane based rolled-up capacitors, which in (b) is shown in their rolled state. In (c) the layer sequence obtained by the self-winding process for inorganic (Case I) and hybrid organic/inorganic (Case II) capacitors is depicted. (d,e) Typical SEM images of nanomembrane-based UCCaps highlighting the high reproducibility of the process.**

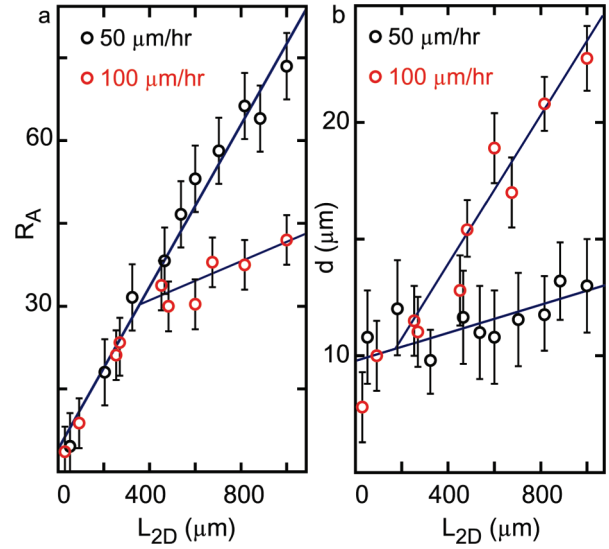


**FIGURE 2. (a) Compactness $R_A$ and (b) diameter $d$ of structures rolled at $s_r$ ~50 $\mu$m/h and $s_r$ ~100 $\mu$m/h as a function of $L_{2D}$. The error bars are calculated from the average of at least 15 rolled-up capacitors. For $L_{2D}$ = 1 mm, an increase of 2.5 (12) $\mu$m of the device external diameter is observed for $s_r$ ~50 (100) $\mu$m/h, respectively.**

rolling of the nanomembrane capacitor shown in Figure 1d results in the reduction of the footprint to ~0.002 mm$^2$, which signifies a compactification of ~25 times of the original unrolled size (0.050 mm$^2$). The footprint shrinkage, quantified by the compactness factor ($R_A$), is evaluated by the ratio of the unrolled ($A_{2D}$) to rolled ($A_{3D}$) device footprint area. The dependence of both $R_A$ and tube diameter ($d$) with the unrolled capacitor length ($L_{2D}$) is plotted in Figure 2a,b.

By increasing $s_r$, the compactness tends to decrease beyond a rolling distance of ~400 $\mu$m, resulting in an evident kink in the figure. For capacitors with $L_{2D}$ = 1 mm, $R_A$ increases almost 2 orders of magnitude by setting $s_r \leq$ 50 $\mu$m/h while for $s_r$ ~100 $\mu$m/h $R_A$ ~45. Independent of $s_r$, the diameter $d$ has the tendency to converge to ~10 $\mu$m as $L_{2D}$ becomes smaller, indicating that the low $R_A$ obtained at $s_r$ ~100 $\mu$m/h can be attributed to loose windings instead of a large initial diameter. The UCCap Ca1 (Figure 3) was obtained by the self-rolling of a 1 mm long nanomembrane into ~25 windings at $s_r$ ~50 $\mu$m/h. Therefore, since the layer thickness $t$ of roughly 40 nm, an increase of ~2 $\mu$m of the external diameter is expected for the final tube shaped UCCap. This estimated value agrees well with the value measured by optical microscopy (see Figure 2b). While in this work we mainly employed planar devices smaller than 1 mm, upscaling seems straightforward; longer and wider capacitor structures can be compacted by the same means. For comparison, by using a multilayer stack procedure for fabricating capacitors with similar electrical characteristics and lateral size of the UCCap in Figure 3, it would be necessary to perform ~60 deposition processes including a minimum of 30 lithographic steps. A yield loss of 3% at each masking step will accumulate to at least 60% loss after the whole fabrication process.[16] For our process, we estimate a maximum final yield loss of 10%.

In addition to reducing the device footprint by the rolling process, the bottom metallic plate mechanically touches the top oxide layer so that the final active capacitor area increases. For a large number of rotations ($N$), this effect is equivalent to connecting two unrolled capacitors in parallel. Figure 4a shows the capacitance increase due to the rolling for Ca1 (Figure 3). By considering the additional contacted area gained by rolling, the capacitance of an UCCap ($C_{3D}$) can be obtained by the relation

$$C_{3D} = C_{2D}\left(2 - \frac{1}{N}\right) \quad (1)$$

where $C_{2D} = \kappa_{OX}\varepsilon_0 A_{2D}/t_{OX}$ is the unrolled device capacitance, and $\kappa_{OX}$ and $t_{OX}$ are the relative dielectric constant and the oxide thickness, respectively (see Supporting Information for



DOI: 10.1021/nl1010367 | *Nano Lett.* **2010,** *10,* 2506–2510

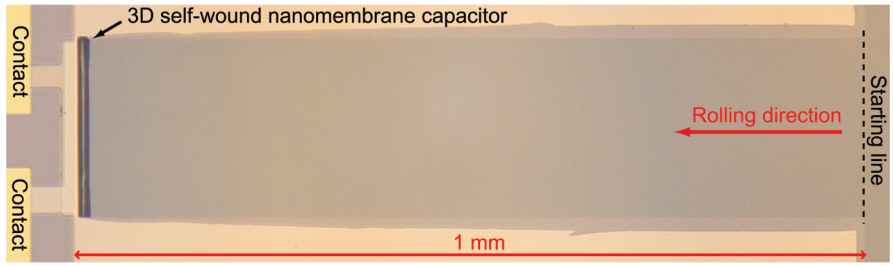


FIGURE 3. Optical image of an UCCap (Ca1) rolled-up from a stripe 1 mm long at ~50 $\mu$m/h into a tube with ~13 $\mu$m diameter. The rolled-up device is almost 2 orders of magnitude smaller than its planar counterpart.

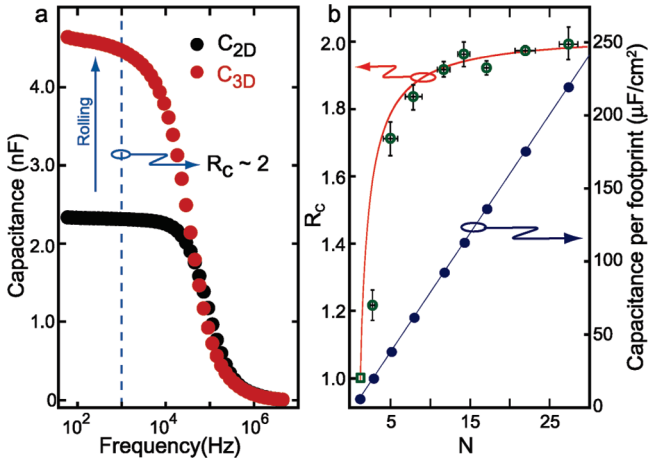


FIGURE 4. (a) Increase of the capacitance going from 2D to 3D structures. (b) The increase of the capacitance per footprint area (right-axis) and $R_c$ with number of windings $N$ (left-axis), which indicates good agreement with the results calculated from eq 1 (red solid line). For $N \gg 1$, the graph further highlights the convergence $R_C \rightarrow 2$.

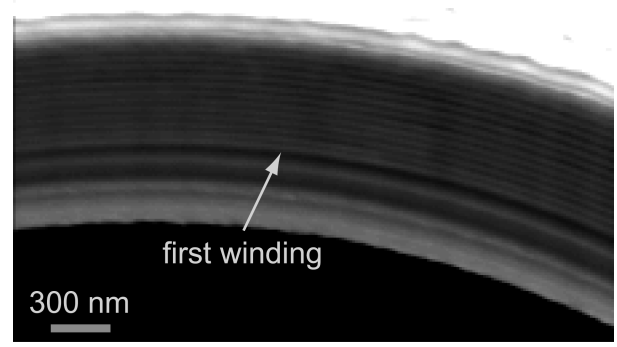


FIGURE 5. Cross-sectional view of an UCCap comprising ~13 windings and rolled from a 600 $\mu$m long planar capacitor.

more details). Up to 5 kHz, both rolled and flat devices have the same $\kappa_{OX} = 9.8 \pm 0.4$, which agrees with the best values previously reported for $Al_2O_3$.[17] Therefore, one attractive rolled-up technology feature is the ability to change both the geometry and the geometric-related parameters of the devices without compromising the structural and electronic integrity of the materials used. By simply self-winding Ca1, the capacitance per footprint area[27] ($C_{sp}$) significantly increases from ~1.3 to ~200 $\mu$F/cm$^2$ (Figure 4b), highlighting the advantage of combining top-down with self-assembly methods. Taking into account the typical $Al_2O_3$ layer density deposited by ALD[18] (~3 g/cm$^3$), the UCCap in Figure 3 exhibits high power density (~2000 W/kg), which is characteristic of electrostatic capacitors, while reaching a specific energy of ~0.55 Wh/kg in the range of supercapacitors.[19] Such a remarkable performance could be further improved by combining high-k oxides, such as $HfO_2$ ($\kappa_{OX}$ ~25) and $TiO_2$ ($\kappa_{OX}$ ~80)[20,21] with larger plate areas. Taking a layer structure similar to that in Figure 1c, the rolling-up of a 4 nm $HfO_2$ capacitor with a planar area of ~20 mm$^2$ would result in a UCCap 300 times smaller and with a capacitance per footprint area of ~3.5 mF/cm$^2$ (~10 mF/cm$^2$ for $TiO_2$).

As shown in Figure 4a–b, at 1 kHz and for $N = 25$, $R_C = C_{3D}/C_{2D}$ converges to 2 and agrees with eq 1 in the limit of $N \gg 1$, which considers the ideal case where a perfect contact between metal and oxide excludes the presence of defects such as loose windings and/or voids. This suggests that disturbed interfaces between consecutive windings do not substantially affect the ratio $R_C$ for $N > 10$. Consequently, the fact that $R_C$ ~2 indicates that a tight binding and an effective mechanical metal/oxide interface can be obtained by accurately controlling the rolling speed and the number of windings. The cross-sectional view of the device in Figure 5 demonstrates the tight windings of the subsequent capacitor/dielectric plates. In fact, the comparison of $R_C$ with the expected value can be used as a nondestructive method to evaluate the winding compactness level after rolling. For those UCCaps rolled at ~100 $\mu$m/h, $R_C$ is found to be roughly 1.4 regardless of $N$.

One of the strongest attributes of this fabrication technique is the capability of preparing 3D ultracompact devices by self-assembly in aqueous solutions. The harmless nature of this media allows us to integrate organic materials into the devices. To demonstrate this advantage, we have self-assembled phosphonic acid anchor groups into the UCCap structure. Such organic molecules have already been employed previously to reduce leakage currents in organic field-effect transistors.[22,23] Figure 1c illustrates the hybrid organic/inorganic UCCap layer structure after the self-assembled monolayer (SAM) incorporation whose electrical characteristics are strongly correlated to the molecule properties, for example, the SAM grown on top of the $Al_2O_3$ layer results in an additional high-gap barrier that helps to control leakage currents.



DOI: 10.1021/nl1010367 | *Nano Lett.* **2010,** *10,* 2506–2510

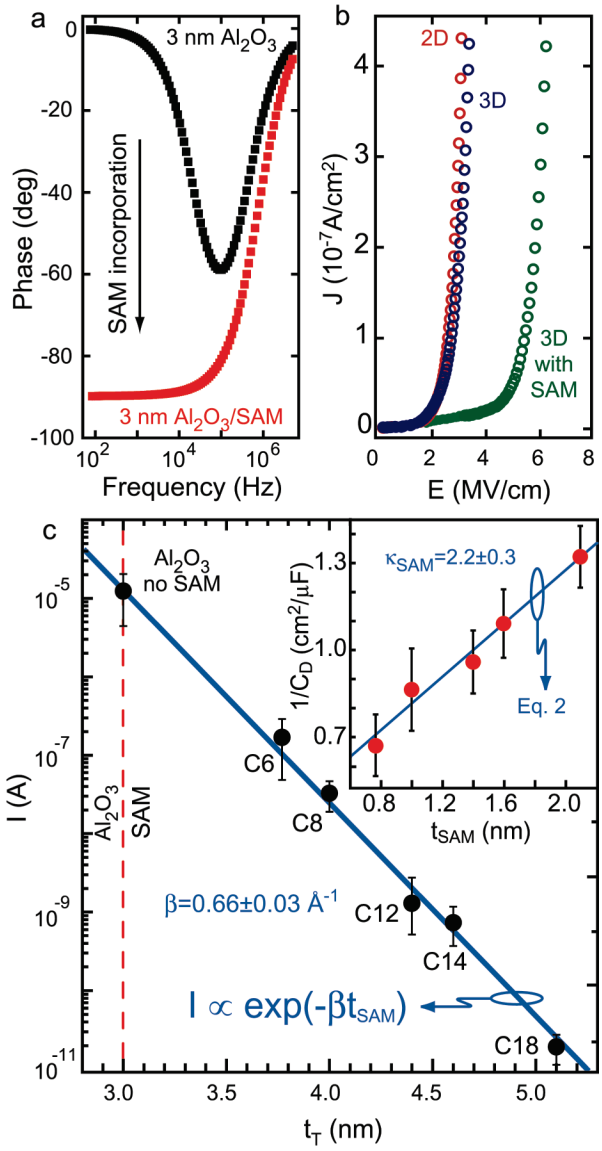


**FIGURE 6. (a) The incorporation of the SAM leads to the recovery of capacitive behavior (a) and an increase in breakdown electric field (b) of UCCaps. In (b), no substantial difference is observed between rolled (3D) and unrolled (2D) devices with 3 nm $Al_2O_3$ (Ca2). For both 2D and 3D capacitors $J$ is found to be $10^{-8}$ A/cm$^2$ under $E \sim 2$ MV/cm. In Ca1, the same $J$ is measured at $E \sim 2.5$ MV/cm for 6.7 nm $Al_2O_3$. (c) The control of the UCCaps electrical properties is demonstrated by the dependence of leakage current with the SAM chain length ($t_{SAM}$). The total dielectric thickness is $t_T = t_{OX} + t_{SAM}$. The upper inset indicates that the device capacitance decreases with increasing SAM chain length.**

As shown in Figure 6a, by using 3 nm of $Al_2O_3$ as a dielectric layer (UCCap Ca2), the charge transport is mainly dominated by resistive currents (phase equals zero at low frequencies). However, after the growth of C18-SAM on the top of this "leaky" $Al_2O_3$, two evident changes are noticed: a phase shift from 0 to −90° indicating a full recovery of the capacitive behavior, and the strong current density ($J$) suppression, allowing an increase of the UCCaps electric field ($E$) operation range by a factor 2.5 (Figure 6b). Additionally, by varying the molecule chain length (from C6- to C18-SAM), we are able to not only suppress $J$ but also control it. Figure 6c shows the dependence of the leakage current ($I$) with the total dielectric thickness ($t_T$) for an applied bias of 1 V. Even by employing molecules with shorter chain lengths, such as C6-SAM,[24] we are able to reduce the capacitor leakage current by over 2 orders of magnitude. The systematic change of the chain length ($t_{SAM}$) in this experimental series furthermore reveals the tunneling character of $I$.[25] The current through the SAM shows an exponential dependence on the barrier width $I \propto \exp(-\beta t_{SAM})$, where $\beta$ is the decay coefficient. From the tunneling model, the parameter $\beta$ is found to be $0.66 \pm 0.03$ Å$^{-1}$, which is in accordance with the accepted values for $\sigma$-saturated molecules.[26]

The equivalent capacitance of the hybrid organic/inorganic UCCap ($C_{EQ}$) is modeled as a series circuit of two capacitors with different dielectric materials, here $Al_2O_3$ and the SAM. Therefore, the capacitance density ($C_D = C_{EQ}/A_{2D}$) can be written as

$$\frac{1}{C_D} = \frac{t_{OX}}{\kappa_{OX}\varepsilon_0} + \frac{1}{\kappa_{SAM}\varepsilon_0} t_{SAM} \qquad (2)$$

where $\kappa_{SAM}$ is the relative dielectric constant of the SAM. The inset in Figure 6c shows the dependence $1/C_D$ vs $t_{SAM}$. By using eq 2 to fit the data, we find $\kappa_{OX} = 9.6 \pm 0.6$ and $\kappa_{SAM} = 2.2 \pm 0.3$ for $t_{OX} = 3$ nm. Both parameters are in good agreement with the values already obtained for Ca1 and with previously reported works,[27] respectively.

In conclusion, we have demonstrated that rolled-up technology is suitable to fabricate self-wound nanomembrane-based capacitors operating at room temperature. To the best of our knowledge, the UCCaps exhibit capacitances per footprint area higher than their state-of-the-art planar counterparts[28−31] and specific energy comparable with supercapacitors. While their small size may limit their application range to low-power systems, we believe that rolled up supercapacitors with high specific energy could find many uses in stand-alone microelectronic systems where other supercapacitor structures would be far too bulky.

Three-dimensional hybrid organic/inorganic UCCaps have been fabricated and characterized confirming the potential of merging molecular with nonmolecular electronics. The integration of organic molecules provides further free parameters to tune the properties and extend the range of applications of the final self-wound device. Replacing the phosphonic acids by magnetic molecules may represent a route toward organic spin-electronics in the near future, the incorporation of solid-state-electrolytes could lead to ultracompact batteries for implantable biomedical systems or on board energy sources for autonomously operating micro/nanorobotic systems[32] in the long term.

**Acknowledgment.** The authors acknowledge Hagen Klauk, Ute Zschieschang, Alex Kleiner, Andrew Buxton, Elliot John



DOI: 10.1021/nl1010367 | *Nano Lett.* **2010,** *10,* 2506–2510

Smith, Gaoshan Huang, Stefan Harazim, Juliane Gabel, Jens Ingolf Mönch, Francesca Cavallo, Juan Diego Arias Espinoza, and Ronny Engelhard for their help and fruitful discussions. J.D.C.G. acknowledges the partial financial support provided by CONICIT, MICIT, and OAICE of the Universidad de Costa Rica. This work is also partially supported by the U.S. Air Force Office of Scientific Research MURI program under Grant FA9550-09-1-0550.

**Supporting Information Available.** Experimental section and additional figures. This material is available free of charge via the Internet at http://pubs.acs.org.

## REFERENCES AND NOTES

(1) Packan, P. A. *Science* **1999**, *285*, 2079.
(2) Cahen, D.; Hodes, G. *Adv. Mater.* **2002**, *14*, 789.
(3) Kim, D.-H.; Rogers, J. A. *ACS Nano* **2009**, *3*, 498.
(4) Schmidt, O. G.; Deneke, C.; Kiravittaya, S.; Songmuang, R.; Heidemeyer, H.; Nakamura, Y.; Zapf-Gottwick, R.; Muller, C.; Jin-Phillipp, N. Y. *IEEE J. Sel. Top. Quantum Electron.* **2002**, *8*, 1025.
(5) Baca, A. J.; Ahn, J.-H.; Sun, Y.; Meitl, M. A.; Menard, E.; Kim, H.-S.; Choi, W. M.; Kim, D.-H.; Huang, Y.; Rogers, J. A. *Angew. Chem., Int. Ed.* **2008**, *47*, 5524.
(6) Roberts, M. M.; Klein, L. J.; Savage, D. E.; Slinker, K. A.; Friesen, M.; Celler, G.; Eriksson, M. A.; Lagally, M. G. *Nat. Mater.* **2006**, *5*, 388.
(7) Whitesides, G. M.; Grzybowski, B. *Science* **2002**, *295*, 2418.
(8) Decher, G. *Science* **1997**, *277*, 1232.
(9) Sun, Y.; Choi, W. M.; Jiang, H.; Huang, Y. Y.; Rogers, J. A. *Nat. Nanotechnol.* **2006**, *1*, 201.
(10) Gracias, D. H.; Tien, J.; Breen, T. L.; Hsu, C.; Whitesides, G. M. *Science* **2000**, *289*, 170.
(11) Jacobs, H. O.; Tao, A. R.; Schwartz, A.; Gracias, D. H.; Whitesides, G. M. *Science* **2002**, *296*, 323.
(12) Schmidt, O. G.; Eberl, K. *Nature* **2001**, *410*, 168.
(13) Stoney, G. G. *Proc. R. Soc. London, Ser. A* **1909**, *82*, 172.
(14) Prinz, V. Y.; Seleznev, V. A.; Gutakovsky, A. K.; Chehovskiy, A. V.; Preobrazhenskii, V. V.; Putyato, M. A.; Gavrilova, T. A. *Physica E* **2000**, *6*, 828.
(15) Mei, Y. F.; Huang, G. S.; Solovev, A. A.; Urena, E. B.; Moench, I.; Ding, F.; Reindl, T.; Fu, R. K. Y.; Chu, P. K.; Schmidt, O. G. *Adv. Mater.* **2008**, *20*, 4085.
(16) Levinson, H. J. *Lithography process control*; SPIE Publications: Bellinghan, MA, 1999.
(17) Wilk, G. D.; Wallace, R. M.; Anthony, J. M. *J. Appl. Phys.* **2001**, *89*, 5243.
(18) Groner, M. D.; Fabreguette, F. H.; Elam, J. W.; George, S. M. *Chem. Mater.* **2004**, *16*, 639.
(19) Winter, M.; Brodd, R. J. *Chem. Rev.* **2004**, *104*, 4245.
(20) Robertson, J. *J. Vac. Sci. Technol., B* **2000**, *18*, 1785.
(21) Robertson, J. *Rep. Prog. Phys.* **2006**, *69*, 327.
(22) Klauk, H.; Zschieschang, U.; Pflaum, J.; Halik, M. *Nature* **2007**, *445*, 745.
(23) Sekitani, T.; Yokota, T.; Zschieschang, U.; Klauk, H.; Bauer, S.; Takeuchi, K.; Takamiya, M.; Sakurai, T.; Someya, T. *Science* **2009**, *329*, 1516.
(24) Spori, D. M.; Venkataraman, N. V.; Tosatti, S. G.; Durmaz, F.; Spencer, N. D.; Zürcher, S. *Langmuir* **2007**, *23*, 8053.
(25) Wang, W.; Lee, T.; Reed, M. *Phys. Rev. B* **2003**, *68*, No. 035416.
(26) Salomon, A.; Cahen, D.; Lindsay, S.; Tomfohr, J.; Engelkes, V. B.; Frisbie, C. D. *Adv. Mater.* **2003**, *15*, 1881.
(27) Fontaine, P.; Goguenheim, D.; Deresmes, D.; Vuillaume, D.; Garet, M.; Rondelez, F. *Appl. Phys. Lett.* **1993**, *62*, 2256.
(28) Banerjee, P.; Perez, I.; Henn-Lecordier, L.; Lee, S. B.; Rubloff, G. W. *Nat. Nanotechnol.* **2009**, *4*, 292.
(29) Klootwijk, J. H.; Jinesh, K. B.; Dekkers, W.; Verhoeven, J. F.; van den Heuvel, F. C.; Kim, H.-D.; Blin, D.; Verheijen, M. A.; Weemaes, R.; Kaiser, M.; Ruigrok, J.; Roozeboom, F. *IEEE Electron Device Lett.* **2008**, *29*, 740.
(30) Kemell, M.; Ritala, M.; Leskela, M.; Ossei-Wusu, E.; Carstensen, J.; Foll, H. *Microelectron. Eng.* **2007**, *84*, 313.
(31) Sohn, J. I.; Kim, Y.-S.; Nam, Ch.; Cho, B. K.; Seong, T.-Y.; Lee, S. *Appl. Phys. Lett.* **2005**, *87*, 123115.
(32) Solovev, A. A.; Mei, Y. F.; Ureña, E. B.; Huang, G. S.; Schmidt, O. G. *Small* **2009**, *5*, 1688.



DOI: 10.1021/nl1010367 | *Nano Lett.* **2010,** *10,* 2506--2510